

See discussions, stats, and author profiles for this publication at: <https://www.researchgate.net/publication/270655896>

# Attenuation of the Early Events of $\alpha$ -Synuclein Aggregation: A Fluorescence Correlation Spectroscopy and Laser Scanning Microscopy Study in the Presence of Surface-Coated Fe<sub>3</sub>O<sub>4</sub> N...

ARTICLE *in* LANGMUIR · JANUARY 2015

Impact Factor: 4.46 · DOI: 10.1021/la503749e · Source: PubMed

---

READS

229

## 6 AUTHORS, INCLUDING:



Nidhi Joshi

Indian Institute of Chemical Biology

5 PUBLICATIONS 59 CITATIONS

[SEE PROFILE](#)



Sujit Basak

University of Massachusetts Medical School

7 PUBLICATIONS 36 CITATIONS

[SEE PROFILE](#)



Anindita Mukhopadhyay

Central Glass and Ceramics Research Institute

14 PUBLICATIONS 351 CITATIONS

[SEE PROFILE](#)



Krishnananda Chattopadhyay

Indian Institute of Chemical Biology

40 PUBLICATIONS 912 CITATIONS

[SEE PROFILE](#)

## Attenuation of the Early Events of $\alpha$ -Synuclein Aggregation: A Fluorescence Correlation Spectroscopy and Laser Scanning Microscopy Study in the Presence of Surface-Coated $\text{Fe}_3\text{O}_4$ Nanoparticles

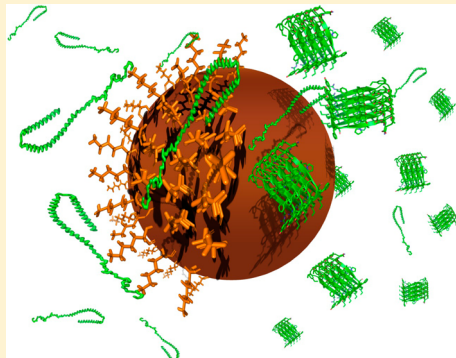
Nidhi Joshi,<sup>§,†</sup> Sujit Basak,<sup>§,†</sup> Sangeeta Kundu,<sup>†</sup> Goutam De,<sup>‡</sup> Anindita Mukhopadhyay,<sup>\*,‡</sup> and Krishnananda Chattopadhyay<sup>\*,†</sup>

<sup>†</sup>Protein Folding and Dynamics Laboratory Structural Biology and Bioinformatics Division, CSIR-Indian Institute of Chemical Biology, 4, Raja S. C. Mullick Road, Kolkata 700032, India

<sup>‡</sup>Nano-Structured Materials Division, CSIR-Central Glass and Ceramics Research Institute, 196, Raja S. C. Mullick Road, Kolkata 700032, India

### S Supporting Information

**ABSTRACT:** The aggregation of  $\alpha$ -synuclein (A-syn) has been implicated in the pathogenesis of Parkinson's disease (PD). Although the early events of aggregation and not the matured amyloid fibrils are believed to be responsible for the toxicity, it has been difficult to probe the formation of early oligomers experimentally. We studied the effect of  $\text{Fe}_3\text{O}_4$  nanoparticle (NP) in the early stage of aggregation of A-syn using fluorescence correlation spectroscopy (FCS) and laser scanning microscopy. The binding between the monomeric protein and NPs was also studied using FCS at single-molecule resolution. Our data showed that the addition of bare  $\text{Fe}_3\text{O}_4$  NPs accelerated the rate of early aggregation, and it did not bind the monomeric A-syn. In contrast, L-lysine (Lys)-coated  $\text{Fe}_3\text{O}_4$  NPs showed strong binding with the monomeric A-syn, inhibiting the early events of aggregation. Lys-coated  $\text{Fe}_3\text{O}_4$  NPs showed significantly less cell toxicity compared with bare  $\text{Fe}_3\text{O}_4$  NPs and can be explored as a possible strategy to develop therapeutic application against PD. To the best of our knowledge, this report is the first example of using a small molecule to attenuate the early (and arguably the most relevant in terms of PD pathogenesis) events of A-syn aggregation.



### INTRODUCTION

The aggregation of  $\alpha$ -synuclein (A-syn), an intrinsically disordered protein (IDP), has been suggested to play key role in Parkinson's disease (PD).<sup>1,2</sup> Although it has been traditionally believed that the generation of the matured amyloid fibrils (or the late stage of protein aggregation) is responsible for the disease, this view has been changing. It has been shown that a number of missense mutations,<sup>3</sup> including A53T, E46K, and A30P, results in increased aggregation rate of protein. It has been found that these autosomal-dominant mutations, instead of accelerating the conversion of oligomers to mature aggregates, speed up the early events of aggregation process (monomer to oligomer formation).<sup>4</sup> There is additional evidence that the early aggregates or oligomers, and not the matured amyloids, are responsible for the pathogenesis.<sup>5</sup>

Although the discovery of a drug (or a vaccine) against PD seems elusive, A-syn remains one of the popular targets for developing therapeutics to inhibit or reverse misfolding and aggregation.<sup>6,7</sup> Unfortunately, there is still no report of a therapeutic agent, which can be targeted toward the early events of A-syn aggregation. This could be due to two reasons: first, it is nontrivial to study the early events of aggregation

using standard biophysical methods, which require comparatively high concentration of aggregates for their detection; second, the dye-based methods, including the binding measurements using thioflavin T (ThT), are better suited for the studies of late events, like the formation of mature fibrils, and not for the early events of aggregation.

A number of experimental techniques has been devoted recently for the direct measurements of the early events of protein aggregation. One of these methods involves the use of environmentally sensitive dyes, including pyrene,<sup>8</sup> amino-naphthalenes,<sup>9</sup> and 3-hydroxychromones.<sup>10</sup> The other method takes advantage of the sensitive detection of fluorescence correlation spectroscopy (FCS) using conventional fluorophores.<sup>11</sup> The use of quantum dots as ultrasensitive detectors for the amyloid formation in live cells has been established.<sup>12</sup>

In this study, we prepared L-lysine (Lys)-coated  $\text{Fe}_3\text{O}_4$  NPs to explore its applications toward the inhibition of the early events of A-syn aggregation. The rationale for using  $\text{Fe}_3\text{O}_4$  NPs

Received: September 22, 2014

Revised: January 1, 2015

comes from their applications in magnetic targeting and also for the potentials they offer as therapeutic agents to cross the blood–brain barrier (BBB).<sup>13</sup> For example, in vitro and in vivo experiments have shown successful transport of lactoferrin-conjugated Fe<sub>3</sub>O<sub>4</sub> NPs across the BBB.<sup>14</sup>

In this study, we chose Lys to modify the bare surface of Fe<sub>3</sub>O<sub>4</sub> NPs. There are several reasons for this. First, the use of bare Fe<sub>3</sub>O<sub>4</sub> NPs may offer undesired conformational effects on the target proteins. In contrast, proper surface modification can reduce this problem and enhance the biocompatibility of Fe<sub>3</sub>O<sub>4</sub> NPs.<sup>15,16</sup> Lys is known for its popular usage as a surface-modifying agent.<sup>17</sup> Second, several natural amino acids, for example, proline, arginine, and Lys have been used as protein stabilizers toward unfolding and aggregation.<sup>18</sup>

In the present study, we aimed to make use of the surface-modifying and aggregation prevention properties of Lys. We used a combination of confocal laser scanning microscopy (LSM) and FCS to visualize and quantify these early aggregates in vitro. FCS measures the diffusional and conformational fluctuations of fluorescently labeled biomolecules at single-molecule resolution.<sup>19</sup> The correlation functions obtained with the FCS measurements can be fit using an optimum model to obtain precise measurements of diffusion time ( $\tau_D$ ). The value of  $\tau_D$  can be used to determine the hydrodynamic radius ( $r_H$ ) of diffusing molecules using Stokes-Einstein formalism (eq 5). The application of FCS to study aggregation of A-syn<sup>11</sup> and amyloid  $\beta$ -peptides<sup>20</sup> has been demonstrated. FCS has been shown to detect low-molecular-weight adduct formation in the case of micellization, and these adducts were not visible by traditional spectroscopic methods. Recently, LSM has been used extensively for monitoring aggregation kinetics of different proteins.<sup>11,21</sup>

We showed that early events of A-syn aggregation were facilitated in the presence of uncoated Fe<sub>3</sub>O<sub>4</sub> NPs. In contrast, the use of Lys-coated Fe<sub>3</sub>O<sub>4</sub> NPs prevented these processes. The use of free Lys as a control did not have a significant effect on the early aggregation of A-syn. We proposed that a competing equilibrium between protein self-association and its binding to the NPs surface may be responsible for the observed results. Lys-coated Fe<sub>3</sub>O<sub>4</sub> NPs showed less cell toxicity compared with bare uncoated Fe<sub>3</sub>O<sub>4</sub> NPs. To the best of our knowledge, this is the first report of the application of Fe<sub>3</sub>O<sub>4</sub> NP-induced inhibition of A-syn aggregation. We also believe that the presented data may have important implications in the design and development of possible therapeutics against PD.

## ■ EXPERIMENTAL SECTION

A detailed description of the experimental materials and methods is provided in the Supporting Information (Additional Text S1, Supporting Information). The characterization of Lys-coated Fe<sub>3</sub>O<sub>4</sub> NPs has also been shown in the Supporting Information (Figure S1, Supporting Information). The concentration of the nanoparticles (bare Fe<sub>3</sub>O<sub>4</sub> NPs and Lys-coated Fe<sub>3</sub>O<sub>4</sub> NPs) was 1 mg/mL unless otherwise mentioned; further details are mentioned in the Supporting Information (Additional Text S1, Supporting Information). Here we have discussed only the relevant details of FCS.

**Fluorescence Correlation Spectroscopy.** The FCS experiments were carried out using the commercial instrument ConfoCor 3 LSM (Carl Zeiss, Evotec, Jena, Germany) using a 40 $\times$  water immersion objective. Samples were excited with an argon laser at 488 nm. A main dichroic filter was used to separate the fluorescence signal from the excited line. The fluorescence signal was collected using two avalanche photodiodes (APDs). A correlator used the photocurrent detected by the APDs to calculate the correlation function. To correct for the

refractive index mismatch between the experimental solution and the immersion liquid, the objective correction collar settings and the heights were adjusted manually.<sup>22</sup> All protein data were normalized with the values of diffusion time ( $\tau_D$ ) obtained with the free dye (Alexa488) measured under identical conditions. The addition of bare or coated Fe<sub>3</sub>O<sub>4</sub> NPs did not result in any significant change in the values of  $\tau_D$  obtained with the free dye.

In a FCS experiment, the fluorescence intensity emitted from a small observation volume is collected as a function of time. The fluorescence intensity fluctuations are recorded as the fluorescently labeled molecules diffusing in and out of this confocal volume. The fluctuation in fluorescence intensity that consists of information on the average number of molecules in the confocal volume, the residence time of molecules, and other photo physical properties can be analyzed using the correlation function.

For a simple solution containing a single diffusing species, the correlation function can be represented as follows

$$G(\tau) = 1 + \frac{1}{N} \cdot \frac{1}{\left(1 + \frac{\tau}{\tau_D}\right)} \cdot \frac{1}{\left(1 + S^2 \frac{\tau}{\tau_D}\right)^{1/2}} \quad (1)$$

where  $\tau_D$  is the characteristic diffusion time of the diffusing species,  $N$  is the average number of particles in the observation volume, and  $S$  is the structural parameter. The dimension of the focal volume is governed by  $r_o$  (focal volume radius) and  $z_o$  (one-half of the distance along the optical path).

For a more complex system<sup>23</sup> involving the aggregated protein molecules, the multicomponent correlation function can be defined by the following equation

$$G(\tau) = 1 + \frac{1}{N} \cdot \sum_i \frac{F_i}{\left(1 + \left(\frac{\tau}{\tau_{D_i}}\right)\right)} \cdot \left( \frac{1}{\left(1 + S^2 \left(\frac{\tau}{\tau_{D_i}}\right)\right)^{1/2}} \right) \quad (2)$$

where  $\tau_{D_i}$  is the diffusion time of the  $i$ th component and  $F_i$  is its amplitude in the correlation function.

As a result of aggregation, the brightness of the diffusing particles is expected to change. We used eq 3 to normalize the change in brightness of the diffusing particles to the correlation function as a result of protein aggregation<sup>23</sup>

$$G(\tau) = \frac{\sum_i^M (B_i)^2 (A_i)^2 g(i)}{\left(\sum_i^M B_i A_i\right)^2} \quad (3)$$

where  $B_i$  is the brightness of  $i$ th species,  $A_i$  is concentration of the  $i$ th species in the observation volume, and  $g(i)$  is the autocorrelation function of  $i$ th species.

For an FCS experiment, the characteristic diffusion time ( $\tau_D$ ) is related to the diffusion coefficient ( $D$ ) by the following equation

$$\tau_D = \frac{\omega^2}{4D} \quad (4)$$

By fitting the experimentally obtained correlation curve using an appropriate model, we can obtain the values of diffusion time ( $\tau_D$ ) and the diffusion coefficient ( $D$ ). The value of the hydrodynamic radius ( $r_H$ ) can be obtained from  $D$  using the Stokes-Einstein formula.

$$D = \frac{kT}{6\pi\eta r_H} \quad (5)$$

**Data Analysis Using the Maximum Entropy Method.** One of the potential problems of FCS data analyses using discrete component method (previously described) comes from the fact that the individual components may influence each other. This is particularly true for a heterogeneous system, like protein aggregation. For this reason, the correlation function data were also analyzed by the maximum entropy method (MEM).<sup>24</sup>

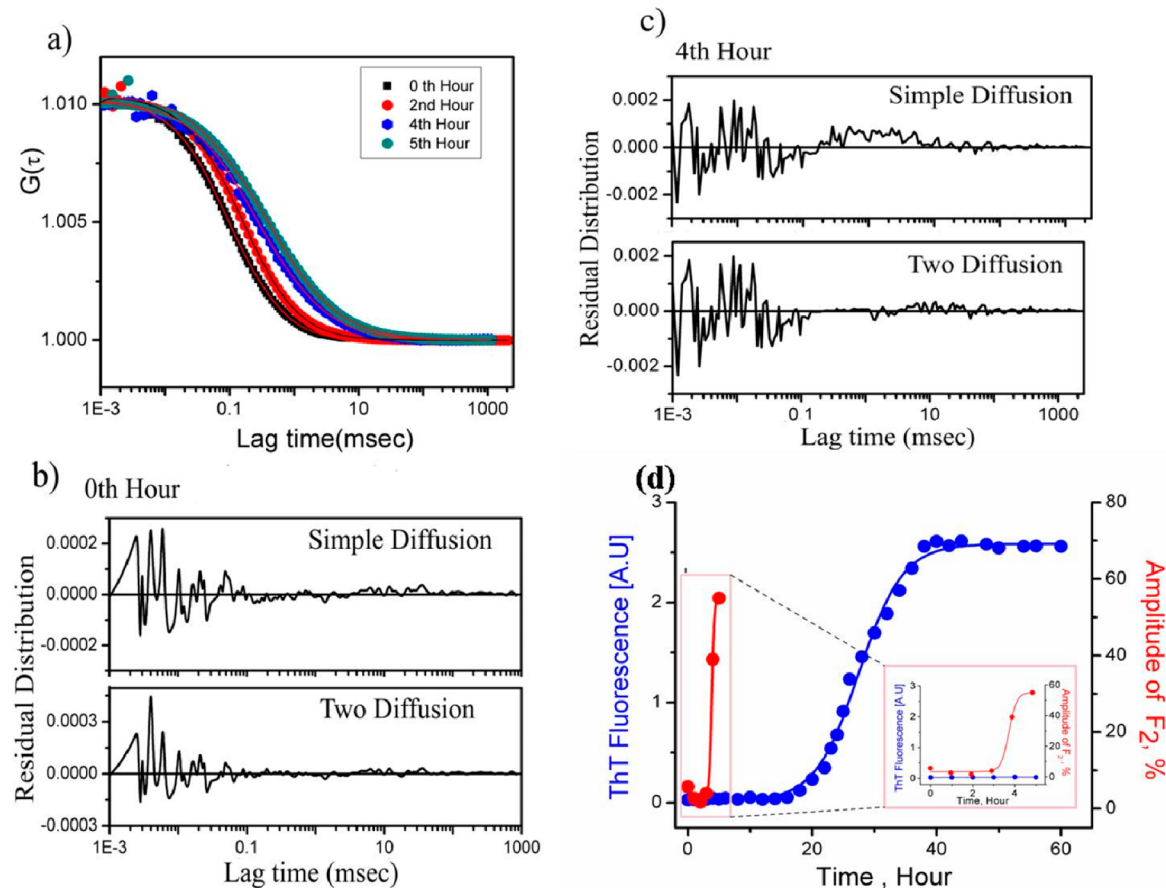


**Figure 1.** (a) As Alexa488Syn was incubated at 37 °C, the correlation functions obtained using FCS experiments started shifting toward the right with time. (b) The correlation function of the monomeric Alexa488Syn could be fit to a model containing a single diffusing species. The goodness of the fit was confirmed by the randomness of the residual distribution. The residual distribution of a two diffusion fit is also shown, which did not show any significant improvement. (c) The residual distributions of the fit of the FCS data obtained at the fourth hour. The single component fit was not adequate, as shown by the nonrandom behavior, while the addition of a second aggregating component yielded a better fit. (d) Comparison of the analytical methods, ThT binding assay and FCS for the detection of early events of A-syn aggregation within the experimental time frame. While ThT binding assay is insensitive to early events of aggregation showing a lag phase, FCS analysis clearly detects the early aggregation of A-syn.

Here the multicomponent correlation function is represented by  $n$  (the number of noninteracting fluorescent species), where each can have a diffusion time of 0.001 to 500 ms. MEMFCS is essentially a model free method, which minimizes  $\chi^2$  and maximizes the entropic value  $S = \sum p_i \ln p_i$  (where  $p_i = \alpha_i \sum \alpha_j$ ) to obtain an optimized fit.

## RESULTS AND DISCUSSION

Because traditional methods of using ThT fluorescence do not detect any change in the lag phase, we used FCS to study the early events of A-syn aggregation at single-molecule resolution. FCS has been used extensively to study protein aggregation by monitoring changes in the diffusion behavior of the aggregating protein molecules.<sup>25</sup> The diffusion of a molecule correlates to its time-averaged dimension. Hence, a well-folded and monomeric protein with a compact shape would yield smaller diffusion time ( $\tau_D$ ) compared with the larger unfolded or aggregated protein. Figure 1a shows typical correlation functions obtained at different time points when Alexa488-labeled G132C mutant of A-syn protein (Alexa488Syn) was incubated in sodium phosphate buffer at pH 7.4. Far-UV circular dichroism (CD) experiments indicated that there was no significant effect of Alexa488 labeling on the secondary structure of the protein (Figure S2, Supporting Information). The temperature was maintained at 37 °C, and the protein

solution was kept under constant stirring. The FCS data obtained at zero time (no aggregation) were fit to an equation, which models a single diffusing species (eq 1). The goodness of the fit was verified by the randomness of the residual distribution (shown in Figure 1b). The addition of a second diffusing component did not improve the fit (the residual distribution shown in Figure 1b). The value of  $\tau_D$  was used to calculate  $r_H$  of the protein using the Stokes-Einstein formalism (eq 5). The calculated value of  $r_H$  (31.5 Å) falls between that expected for a folded protein in aqueous buffer (19.9 Å) and that expected for an unfolded protein in the presence of a chemical denaturant (36.9 Å) (Additional Text S2, Supporting Information), confirming the natively unfolded nature of the protein.

As the protein was incubated at 37 °C, the values of  $r_H$  deviated significantly from the value observed with the monomeric protein. This was evident from the large shift in the correlation function to the right, as the time of incubation increased (Figure 1a). In addition, the observed correlation functions could not be fit to a single component model, which was evident from the nonrandom behavior in the residual distribution analyses (Figure 1c). Instead, the correlation function data were fit successfully to a sum of two diffusing components, the fast and slow components representing the

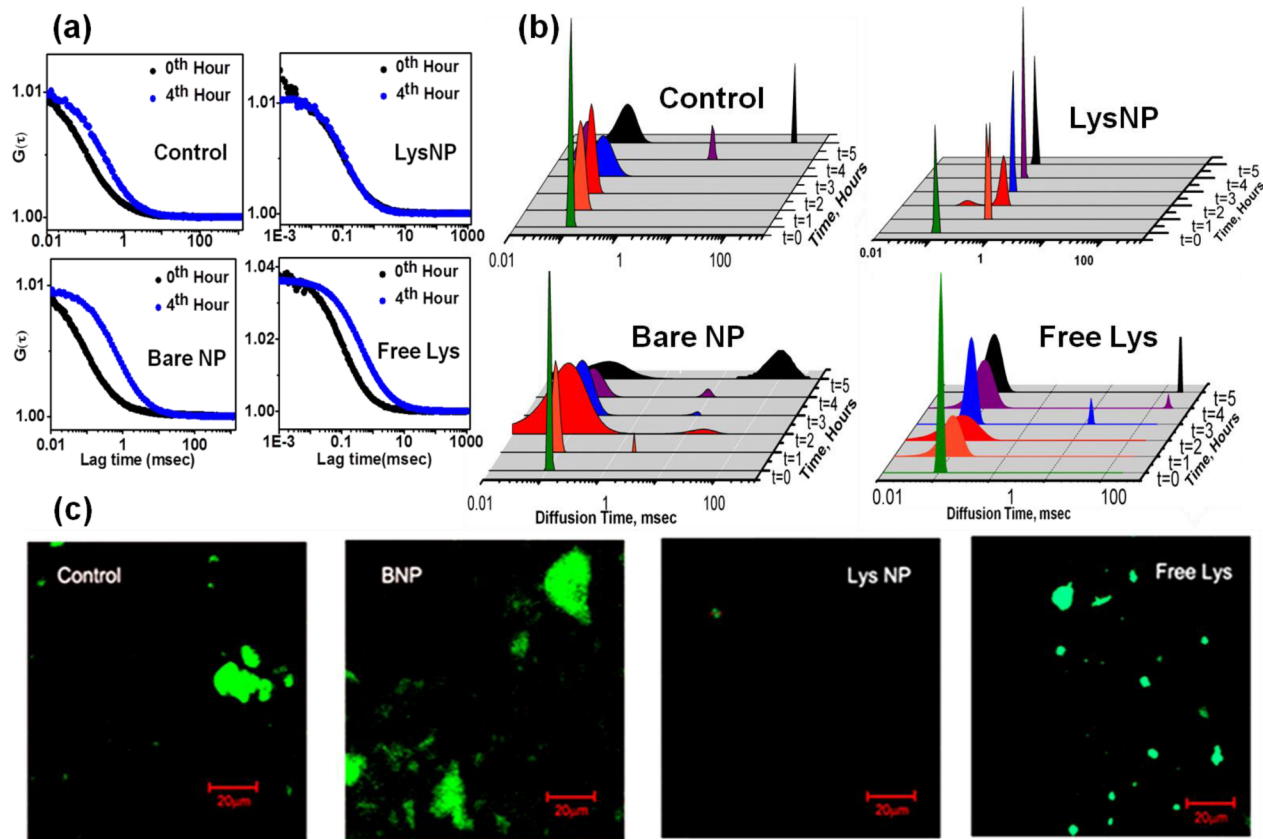


**Figure 2.** (a) Correlation functions obtained by the FCS experiments with Alexa488Syn after 0 (black) and 4 h (blue) of incubation in the presence of bare (BNP) and Lys-coated  $\text{Fe}_3\text{O}_4$  NPs. The data obtained in the absence of any NPs (control) and in the presence of Lys (Free Lys) are also shown. (b) MEM profiles obtained at different hours of incubation in the absence and presence of bare and coated  $\text{Fe}_3\text{O}_4$  NPs. (c) Confocal microscopy images obtained after 4 h of incubation in the absence and presence of NPs.

diffusion of monomer and aggregated species, respectively. The residual distribution of the two-component fit is also shown in Figure 1c. The aggregation kinetics monitored by ThT fluorescence showed no increase in the emission intensity during the early stages of aggregation (Figure 1d). Under this condition (4 h of incubation at 37 °C), no ThT binding was observed, indicating the absence of amyloid fibril formation (Figure 1d). It may be noted that the use of MFC probe has been shown to provide detailed information about the continuous nature of A-syn aggregation.<sup>10</sup>

Because it is difficult to directly monitor the early events by conventional methods, there are controversies regarding the nature of the early aggregates. However, the formation of toxic oligomeric species early in the aggregation has been shown.<sup>4</sup> Further support of the formation of oligomeric species has been provided by FRET<sup>11</sup> (carried out at <4 h) and AFM results<sup>10</sup> (at 6 h). In addition, the presence of dimers and early oligomers has been shown by mass spectroscopy.<sup>26</sup> However, it should be noted that the process of aggregation (both the early and late events) is heterogeneous, and hence the presence of different species of varying conformation is possible. The formation of different morphologies in the late events of aggregation has been shown.<sup>27</sup>

The early aggregation of Alexa488Syn was monitored using FCS in the presence of bare and Lys-coated  $\text{Fe}_3\text{O}_4$  NPs. FCS experiments were also carried out in the absence of any NPs (as control) and in the presence of free Lys. The correlation functions at two different time points were shown for all of

these previously described experiments (Figure 2a). Figure 2a suggested that the extent of early aggregation was higher for Alexa488Syn in the presence of bare  $\text{Fe}_3\text{O}_4$  NPs compared with that observed in the absence of NPs. This was evident from the larger shift of the correlation function at the fourth hour in the presence of bare  $\text{Fe}_3\text{O}_4$  NPs (Figure 2a). In contrast, the presence of Lys-coated  $\text{Fe}_3\text{O}_4$  NPs inhibited the aggregation of Alexa488Syn significantly. This was clearly observed in Figure 2a, which showed almost complete overlap of the correlation functions obtained at the zeroth and fourth hours. The addition of free Lys (not tethered to the nanoparticle) did not seem to have any significant effect, and the data were similar to that obtained without any NPs (Figure 2a).

The correlation function data were independently analyzed using the model-free MEM, and the results are shown in Figure 2b. Identical to the results obtained with the discrete analyses previously described, MEM fittings of the monomeric Alexa488Syn suggested the presence of one  $\tau_D$  distribution. MEM profiles started becoming broader with the increase in time of incubation at 37 °C and eventually started forming two separate distribution profiles. The broadening of MEM distribution presumably represents the increase in the conformational heterogeneity as the aggregation proceeds. It was evident from Figure 2b that the appearance of a second distribution profile, which represented the aggregated component, was initiated faster in the presence of bare  $\text{Fe}_3\text{O}_4$  NPs. In contrast, a second distribution profile could not be observed (was insignificant) in the presence of Lys-coated  $\text{Fe}_3\text{O}_4$  NPs.

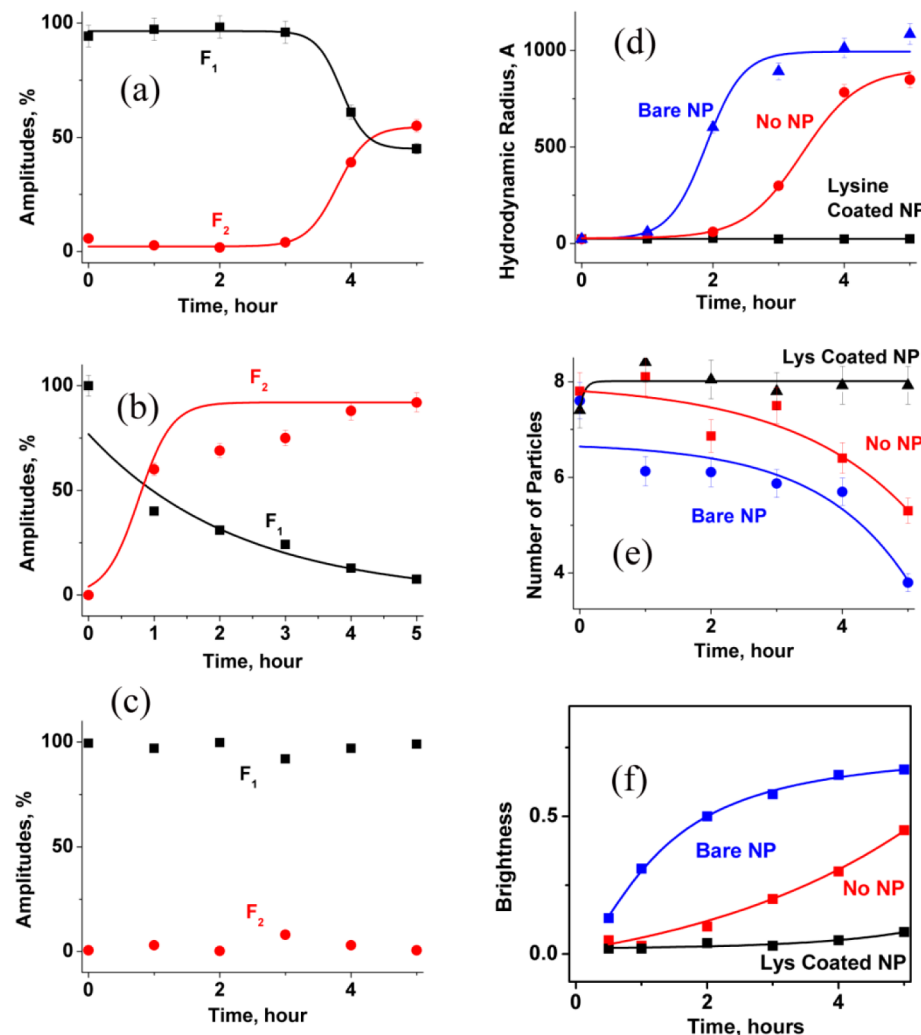


**Figure 3.** Correlation functions obtained by the FCS experiments with Alexa488Syn were fit using a two diffusing components model, and this Figure shows the variations of different parameters with incubation time: the amplitudes of the fast (black) and slow (red) components (a) in the absence of  $\text{Fe}_3\text{O}_4$  NPs, (b) in the presence of bare  $\text{Fe}_3\text{O}_4$  NPs, and (c) in the presence of Lys-coated  $\text{Fe}_3\text{O}_4$  NPs; (d) the values of diffusion time for the slow component, (e) the number of particles; and (f) the brightness of the slow component in the absence (red) and presence of bare (blue) and Lys-coated (black)  $\text{Fe}_3\text{O}_4$  NPs.

The addition of free Lys did not have significant effects on the early aggregation (Figure 2b).

Confocal imaging has been used for the direct visualization of Alexa488Syn early aggregates under different solution conditions. The confocal images were shown at the fourth hour of incubation in the absence and presence of bare and Lys coated  $\text{Fe}_3\text{O}_4$  NPs (Figure 2c). The LSM images obtained with zero hour along with other incubation time points are shown in Figure S3 (Supporting Information). A comparison between the control (no NPs) and the sample containing the bare  $\text{Fe}_3\text{O}_4$  NPs suggests that the early aggregation is higher in the latter solution condition than in the former one (Figure 2c and Figure S3 in the Supporting Information). Large aggregates were observed at the fourth hour of incubation, in both the absence and presence of bare  $\text{Fe}_3\text{O}_4$  NPs, although the accumulation of larger aggregates was greater with the bare  $\text{Fe}_3\text{O}_4$  NPs (Figure 2c and Figure S3 in the Supporting Information). Similarly, confocal images of the protein incubated with Lys-coated  $\text{Fe}_3\text{O}_4$  NPs and with free Lys were taken. A large decrease in the aggregation of Alexa488Syn could be noted in the presence of Lys-coated  $\text{Fe}_3\text{O}_4$  NPs (Figure 2c

and Figure S3 in the Supporting Information). It was quite obvious that whereas control (in the absence of NPs) showed the presence of large sized aggregates, free Lys led to more scattered and presumably smaller aggregates (Figure 2c and Figure S3 in the Supporting Information). These results supported the FCS data and confirmed the fact that the prevention or the deceleration of Alexa488Syn aggregation in the presence of Lys-coated  $\text{Fe}_3\text{O}_4$  NPs was not a manifestation of the Lys alone but was a result of its linkage with NPs surface.

As previously mentioned, the use of multicomponent diffusion model was needed to fit the correlation functions of Alexa488Syn under aggregating conditions. The fast component ( $\tau_{D1}$ ) corresponded to the monomeric protein, while the slow component ( $\tau_{D2}$ ) represented the aggregated proteins. Their amplitudes ( $F_1$  and  $F_2$ ) corresponded to their relative populations. As the protein aggregated with time, the contribution of  $F_2$  increased at the expense of  $F_1$ . The variations of  $F_1$  and  $F_2$ , which represented the change in the relative amplitudes of the monomer and aggregates, were plotted with time in the absence and presence of bare and Lys-coated  $\text{Fe}_3\text{O}_4$  NPs (Figure 3a–c). Additionally, the variations of

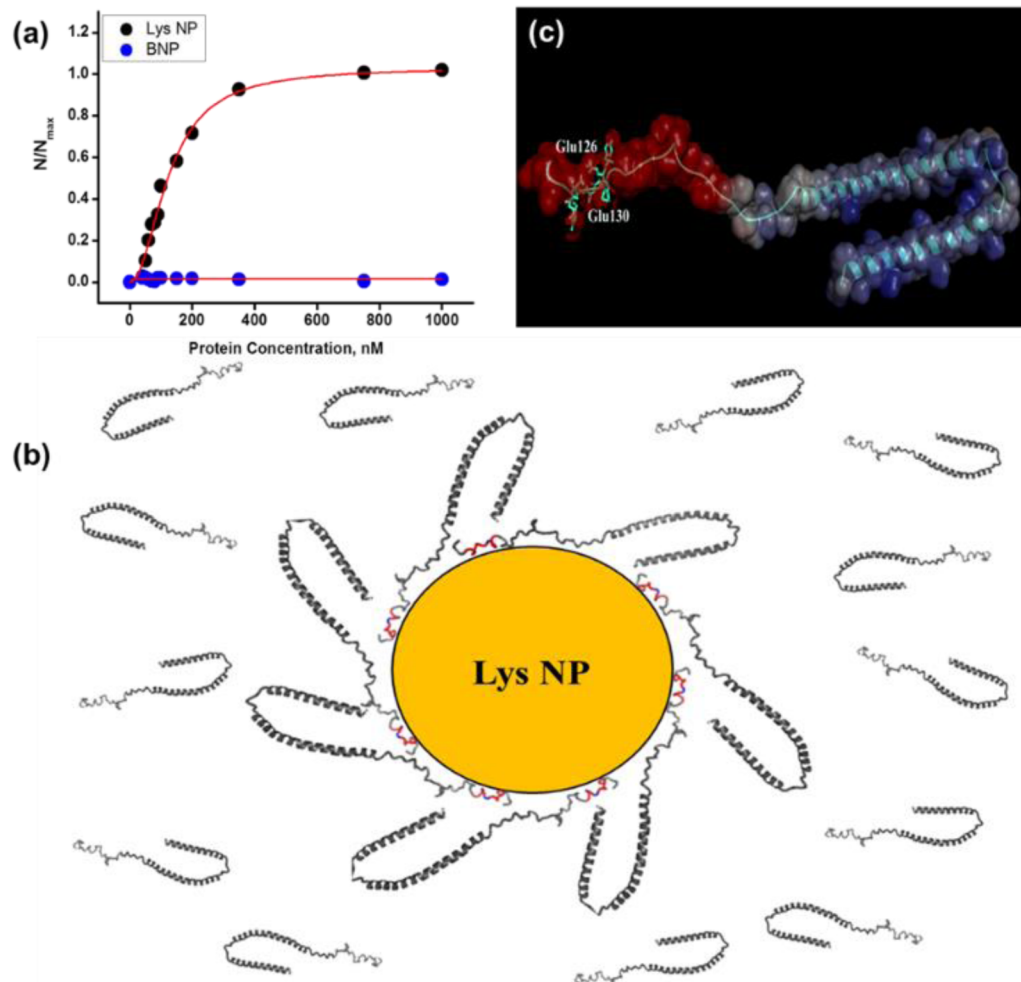


**Figure 4.** (a) Determination of binding constant for the bare (blue) and Lys-coated (black)  $\text{Fe}_3\text{O}_4$  NPs. Here  $N$  is the number of proteins interacting with the NPs along with change in the concentration of the protein and  $N_{\max}$  is the maximum number of proteins interacting with the NPs. (b) Pictorial representation of A-syn corona on the surface of a molecule of Lys-coated  $\text{Fe}_3\text{O}_4$  NPs. While some of the proteins are associated with the Lys-coated  $\text{Fe}_3\text{O}_4$  NPs, some free proteins are also shown that have not yet bound. The interacting C-terminal region has been colored red. Panel c shows the negatively charged pocket where the Lys-coated  $\text{Fe}_3\text{O}_4$  NPs are expected to bind. The negatively charged regions are shown in red, while the blue color is used for the positively charged regions.

$\tau_{D2}$ , which qualitatively represented the size of the aggregates, are plotted with the incubation time under these solution conditions (Figure 3d). The data clearly showed that the presence of bare  $\text{Fe}_3\text{O}_4$  NPs increased the rate of early aggregation, while the presence of Lys-coated  $\text{Fe}_3\text{O}_4$  NPs inhibited the early events of aggregation. Because the process of aggregation results in the association of two or more molecules, this process should decrease the number of molecules ( $N$ ) and increase their brightness. It was observed that the value of  $N$  decreased in the case of control and in the presence of bare  $\text{Fe}_3\text{O}_4$  NPs to different magnitudes (Figure 3e), accompanied by an increase in the brightness of the aggregated Alexa488Syn (Figure 3f), but the value of  $N$  as well as the brightness of protein molecules remained more or less unchanged in the presence of Lys-coated  $\text{Fe}_3\text{O}_4$  NPs (Figure 3e,f). The relative change of both these parameters (Figure 3e,f) also confirmed that the addition of Lys-coated  $\text{Fe}_3\text{O}_4$  NPs strongly inhibited Alexa488Syn aggregation.

FCS experiments were carried out to measure the binding between Alexa488Syn and  $\text{Fe}_3\text{O}_4$  NPs by measuring the values of  $\tau_D$  of the monomeric protein in the presence of bare and

Lys-coated  $\text{Fe}_3\text{O}_4$  NPs (Figure 4a). The values of  $\tau_D$  corresponding to Alexa488Syn increased in the presence of Lys-coated  $\text{Fe}_3\text{O}_4$  NPs, and the dissociation constant ( $K_d$ ) was calculated using the eq S8 in the Supporting Information (Figure 4a). Further details of the used equation S8 and the derivation have been provided as Additional Text S3 (Supporting Information). Relatively stronger and cooperative binding between Lys-coated  $\text{Fe}_3\text{O}_4$  NPs and Alexa488Syn was observed, and the values of dissociation constant ( $K_d$ ) and cooperativity were found to be  $1.25 \times 10^{-4}$  mM and 1.8, respectively. Strong binding between Calmodulin, a calcium-binding protein, and  $\text{Fe}_3\text{O}_4$  NPs ( $K_d$  of  $0.015 \mu\text{M}$ ) has been reported before.<sup>28</sup> We have also calculated the maximum number of proteins that can bind to the Lys-coated  $\text{Fe}_3\text{O}_4$  NPs (Additional Text S3, Supporting Information). It was calculated that  $\sim 35$  protein molecules can associate with a single Lys-coated  $\text{Fe}_3\text{O}_4$  NPs. In contrast, the presence of bare  $\text{Fe}_3\text{O}_4$  NPs did not show any increase in  $\tau_D$ , indicating no significant binding with Alexa488Syn. The addition of free Lys did not show any change in  $\tau_D$ . We confirmed that the extrinsic labeling did not affect the binding significantly, as binding experiments

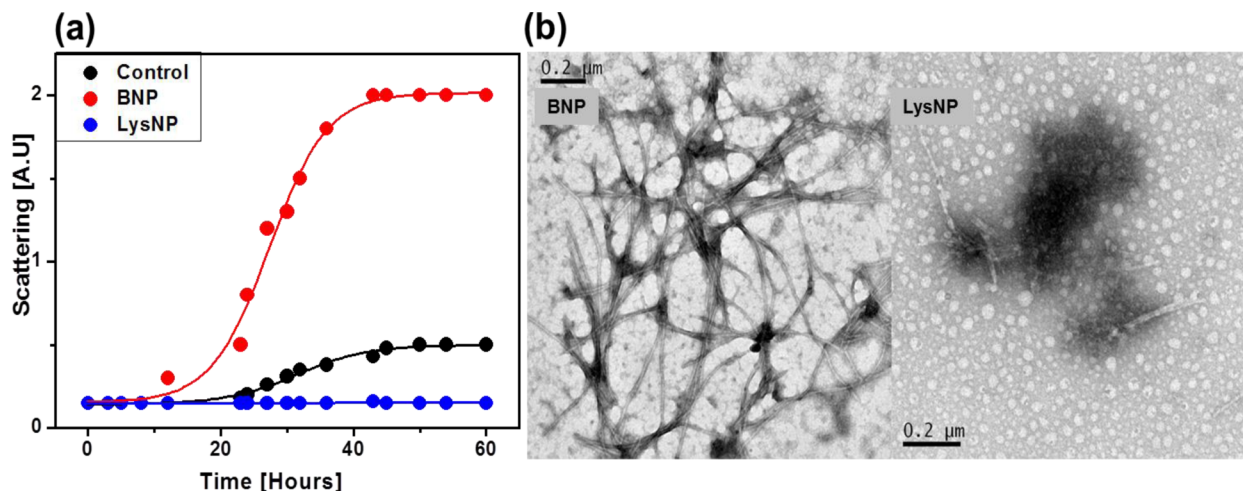


**Figure 5.** (a) Measurements of the late stage of A-syn aggregation in the absence (black) and presence of  $\text{Fe}_3\text{O}_4$  NPs. The data in the presence of bare and Lys-coated  $\text{Fe}_3\text{O}_4$  NPs are shown using red and blue colors, respectively. The data clearly show that the presence of bare  $\text{Fe}_3\text{O}_4$  NPs favored the formation of late stage aggregation, while Lys-coated  $\text{Fe}_3\text{O}_4$  NPs prevented it. (b) TEM micrograph showing the formation of mature fibrils in the presence of bare and Lys-coated  $\text{Fe}_3\text{O}_4$  NPs. In the presence of bare  $\text{Fe}_3\text{O}_4$  NPs, large fibrils of  $25 \pm 5$  nm diameter were found in abundance (left image, marked as BNP). In contrast, the extent of fibrillation was found to be significantly low in the presence of Lys-coated  $\text{Fe}_3\text{O}_4$  NPs (right image, marked as LysNP). Both images were shown using identical scale for easy comparison.

with unlabeled A-syn using tyrosine fluorescence (Figure S4, Supporting Information) yield similar  $K_d$  values ( $4.7 \times 10^{-4}$  mM with Lys-coated  $\text{Fe}_3\text{O}_4$  NPs).

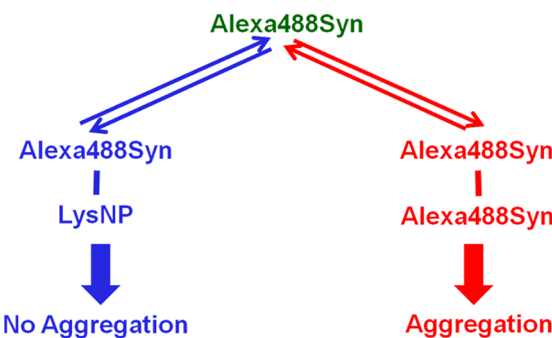
Cell toxicity of these NPs was checked using flow cytometry analysis. NP-treated SH-SY5Y cells showed two different effects (fluorescence activated cell sorting (FACS) data, Figure S5, Supporting Information). While bare  $\text{Fe}_3\text{O}_4$  NPs led to the early and late apoptosis of the cells (Quadrants Q2 and Q4, respectively), Lys-coated  $\text{Fe}_3\text{O}_4$  NPs were able to suppress this effect. About 7.4% (early and late apoptosis collectively, Q2+Q4) cells were found to undergo apoptosis in the presence of bare  $\text{Fe}_3\text{O}_4$  NPs against only 1.9% cells in the presence of Lys-coated  $\text{Fe}_3\text{O}_4$  NPs. This is expected because  $\text{Fe}_3\text{O}_4$  NPs have been shown to induce ROS production and thus may lead to oxidative stress.<sup>29</sup> Proper surface functionalization with biocompatible shells or coating with a polymer may alleviate such harmful effects.<sup>30</sup>

It has been proposed recently that the early oligomers, and not the mature fibrils, may be responsible for the pathogenesis of neurodegeneration.<sup>5,31,32</sup> However, it is difficult to study the early events of aggregation using standard biophysical methods. We used FCS as the principal technique in this study because of its application to monitor the early events of aggregation.<sup>11</sup> The present data showed that FCS can monitor the formation of aggregated species at the early time points of aggregation kinetics, under which condition no ThT binding could be observed (Figure 1d). In addition, we used light scattering and transmission electron microscopy (TEM) to study the effects of these  $\text{Fe}_3\text{O}_4$  NPs on the late events (the formation of amyloid fibrils) (Figure 5a,b). We chose light scattering over ThT fluorescence because the presence of  $\text{Fe}_3\text{O}_4$  NPs quenched ThT fluorescence, leading to complications in fluorescence data analyses. Nevertheless, we compared the ThT fluorescence data and light-scattering results in the absence of  $\text{Fe}_3\text{O}_4$  NPs and found that they represented similar events (Figure S6, Supporting Information). Both light-scattering and TEM data clearly show that the effect of NPs is similar for both early and late stages of aggregation (Figure 5). Similar to what was observed with the early events of aggregation, the presence of

bare and Lys-coated  $\text{Fe}_3\text{O}_4$  NPs favored and inhibited the late stages of aggregation, respectively (Figure 5).

The presence of NPs has been shown to affect the aggregation of different proteins, and these effects vary depending on the nature of NPs. Copolymeric NPs accelerate the aggregation of  $\beta$ 2-microglobulin by promoting nucleation on the NPs surface, while they play inhibitory roles in the aggregation of  $\beta$ -amyloid peptide.<sup>16,33–35</sup> It is also shown that the formation of amyloid fibrils and the effects of a NPs depend on the stability of the protein.<sup>34</sup> On the basis of the previous literatures and the data presented in this paper, we are proposing the mechanism in Scheme 1 to describe the results obtained with Lys-coated  $\text{Fe}_3\text{O}_4$  NPs.

#### Scheme 1



In essence, this mechanism considers a competition between binding of Alexa488Syn to itself (self-association) and to NPs surface (protein–NPs interaction). It can be noted that the primary structure of A-syn consists of two major domains. A lipid binding domain comprises 1–102 residues spanning N-terminal region (positively charged), the central region (hydrophobic core), and a C-terminal end, which is highly acidic in nature. The C-terminal of the protein is believed to remain unstructured in its monomeric as well as in fibrillar forms.<sup>36</sup> It can be assumed that the strong binding of the positively charged Lys-coated  $\text{Fe}_3\text{O}_4$  NPs with Alexa488Syn

(established by the  $K_d$  value obtained in the present study) may be mediated by the negatively charged C-terminal of the protein. To get further insights into this, we carried out docking calculation using the solution NMR structure of A-syn and Lys (Additional Text S4, Supporting Information), which suggested that the binding of Lys through the C-terminal of the protein is the most energetically favorable mode of interaction. A cartoon representation of the protein corona around the Lys-coated  $\text{Fe}_3\text{O}_4$  NPs has been shown in Figure 4b. Moreover, we also measured the zeta potential of Lys-coated  $\text{Fe}_3\text{O}_4$  NPs, which was found to be +26 mV (Figure S7, Supporting Information). Because the positive charge of Lys is still very prominent when it is attached to the NPs, we assumed that the data obtained from the docking studies (where free Lys, and not the NPs, was employed to search for a proper interacting site on A-syn) could be extrapolated to qualitatively interpret our findings. Thus, a pocket that is rich in negatively charged residues (like Glu130, Glu131, Glu126, and Asp135) may be involved in the "Lys-coated  $\text{Fe}_3\text{O}_4$  NPs-A-syn" association (Figure 4c) and the subsequent mitigation of protein aggregation. The docking-related details and the values of free energy of binding have been discussed in the additional Text S3, Supporting Information. The efficient binding between Lys-coated  $\text{Fe}_3\text{O}_4$  NPs and A-syn monomer facilitates the left side of the above equilibrium (Scheme 1) inhibiting the self-association between the A-syn monomers.

The sigmoidal nature of aggregation and the presence of the lag phase have been discussed using several molecular models.<sup>37</sup> Two kinds of molecular contacts (fibrillar and other) between protein or peptide units have been assumed, with the fibrillar contacts on average surviving longer than the other contacts.<sup>37</sup> Although the present data do not directly probe this, it can be speculated that the coated NPs with stronger affinity toward the protein (like Lys-coated  $\text{Fe}_3\text{O}_4$  NPs in the present case) can influence these contact formations, by modulating their relative life times. It is likely that these NPs can bind efficiently to low abundant multimeric species, thus destabilizing them.<sup>34</sup> This destabilization effect of strongly bound NPs toward the multimers and more favored formation of the monomeric species would inhibit both the early and late stage of aggregation, which is observed in the present results.

However, the above binding versus aggregation hypothesis (Scheme 1) does not explain the relative increase in the early aggregation in the presence of bare  $\text{Fe}_3\text{O}_4$  NPs. Our data have shown that the protein does not bind to bare  $\text{Fe}_3\text{O}_4$  NPs (Figure 4a). This is expected because the negative charge (-30 mV) of the bare  $\text{Fe}_3\text{O}_4$  NPs, which has been established by the zeta potential measurements,<sup>38</sup> would not lead to any favorable interaction with the acidic C-terminal of the protein. The lack of binding should ensure that the protein aggregates with identical rate and extent compared with a solution condition, which does not contain any NPs. To summarize, the binding versus aggregation hypothesis effectively predicts no or minimum effect of the bare  $\text{Fe}_3\text{O}_4$  NPs on the aggregation behavior of A-syn. In contrast, the present data show a significant enhancement of the aggregation behavior of A-syn induced by bare  $\text{Fe}_3\text{O}_4$  NPs. Although a stable and efficient binding can be ruled out between Alexa488Syn and bare  $\text{Fe}_3\text{O}_4$  NPs, a transient and unstable binding between the positively charged N-terminal of the protein and the negative surface of bare  $\text{Fe}_3\text{O}_4$  NPs may be considered. Three possible scenarios can explain the enhancement of amyloid formation kinetics observed in the case of A-syn in the presence of weakly

interacting bare  $\text{Fe}_3\text{O}_4$  NPs. First, as previously discussed,<sup>34</sup> a weak interaction ensures no structural loss of the protein in the presence of NPs. In this scenario, the enhancement of the aggregation rate may occur due to the crowding effect imposed on the weakly adsorbed protein at the NPs surface. In the second scenario, we considered the possibility that although the transient interaction is not stabilized because of overall negative charge of the protein at pH 7.4 (-9),<sup>39</sup> it may be sufficient enough for the protein to be exposed to the Fe(II) and Fe(III) ions, which are available in abundance at NPs surface. The support of this hypothesis comes from independent FCS experiments in the presence of excess Fe(II) and Fe(III) salts. The results showed that the presence of both Fe(II) and Fe(III) increased the rate and extent of Alexa488Syn aggregation (Figure S8, Supporting Information). We coated the surface using a known protein repellent, which would further discourage even transient interaction with the protein. We have chosen 10 kD polyethylene glycol (PEG10kD) for this purpose. PEG is known for its protein repellent behavior on surface because of its hydrophilicity, chain mobility, and less ionic charge.<sup>40</sup> Protein-repellent properties of PEG have been extensively studied using  $\text{Fe}_3\text{O}_4$ <sup>41–43</sup> and nanostructured silica-based interfaces.<sup>44</sup> We have monitored the aggregation of Alexa488Syn in the presence of PEG10kD-coated  $\text{Fe}_3\text{O}_4$  NPs, and the data are shown in Figure S8 (Supporting Information). In the presence of PEG10KD-coated NPs, the aggregation kinetics remained similar to that observed in the absence of NPs. The increase in the aggregation, which was observed in the bare  $\text{Fe}_3\text{O}_4$  NPs, was found to be absent in the presence of PEG10KD-coated  $\text{Fe}_3\text{O}_4$  NPs. Finally, it is also possible that an alteration in the ionic strength of the solution might have led to the increased aggregation of the protein. It is already known that  $\text{Fe}_3\text{O}_4$  NPs are capable of altering the ionic strength of the local surroundings and hence leading to uncalled-for effects.<sup>45</sup>

## ASSOCIATED CONTENT

### S Supporting Information

Additional texts containing detailed experimental methods, hydrodynamic radius determination, dissociation constant determination, and docking calculations. Characterization of Lys coated  $\text{Fe}_3\text{O}_4$  NPs. Far-UV CD experiments on the unlabeled and labeled A-syn. LSM images of A-syn aggregation obtained at different hours of incubation. Fluorescence quenching experiment to show the binding of Lys coated  $\text{Fe}_3\text{O}_4$  NPs with the protein. Flow cytometry analysis of SH-SY5Y cell line in the presence of bare  $\text{Fe}_3\text{O}_4$  NPs and in the presence of Lys coated  $\text{Fe}_3\text{O}_4$  NPs. Comparison between fluorescence light scattering and ThT binding assay. Zeta potential of Lys coated  $\text{Fe}_3\text{O}_4$  NPs showing positive value with a peak maximum at +26 mV. Aggregation kinetics of the protein in the presence of Fe(II) and Fe(III) salts. This material is available free of charge via the Internet at <http://pubs.acs.org>.

## AUTHOR INFORMATION

### Corresponding Authors

\*E-mail: krish@iicb.res.in.

\*E-mail: anindita@cgcri.res.in.

### Author Contributions

<sup>§</sup>N.J. and S.B. contributed equally.

### Notes

The authors declare no competing financial interest.

## ACKNOWLEDGMENTS

We thank Prof. Sudipta Maiti of the Tata Institute of Fundamental Research for the MEMFCS software. K.C. thanks CSIR Network Project Grant, MIND, for the funding support. A.M. thanks DST Woman Scientists Program for the fellowship. The Director, CSIR-IICB has been gratefully acknowledged for his help and encouragements.

## REFERENCES

- (1) Fink, A. L. The aggregation and fibrillation of alpha-synuclein. *Acc. Chem. Res.* **2006**, *39* (9), 628–34.
- (2) Hejjaoui, M.; Haj-Yahya, M.; Kumar, K. S. A.; Brik, A.; Lashuel, H. A. Towards Elucidation of the Role of Ubiquitination in the Pathogenesis of Parkinson's Disease with Semisynthetic Ubiquitinated  $\alpha$ -Synuclein. *Angew. Chem., Int. Ed.* **2011**, *50* (2), 405–409.
- (3) Polymeropoulos, M. H.; Lavedan, C.; Leroy, E.; Ide, S. E.; Dehejia, A.; Dutra, A.; Pike, B.; Root, H.; Rubenstein, J.; Boyer, R.; Stenroos, E. S.; Chandrasekharappa, S.; Athanasiadou, A.; Papapetropoulos, T.; Johnson, W. G.; Lazzarini, A. M.; Duvoisin, R. C.; Di Iorio, G.; Golbe, L. I.; Nussbaum, R. L. Mutation in the alpha-synuclein gene identified in families with Parkinson's disease. *Science* **1997**, *276* (5321), 2045–2047.
- (4) Conway, K. A.; Lee, S. J.; Rochet, J. C.; Ding, T. T.; Williamson, R. E.; Lansbury, P. T., Jr. Acceleration of oligomerization, not fibrillization, is a shared property of both alpha-synuclein mutations linked to early-onset Parkinson's disease: implications for pathogenesis and therapy. *Proc. Natl. Acad. Sci. U. S. A.* **2000**, *97* (2), 571–576.
- (5) Glabe, C. G. Common mechanisms of amyloid oligomer pathogenesis in degenerative disease. *Neurobiol. Aging* **2006**, *27* (4), 570–575.
- (6) Ikenoue, T.; Lee, Y. H.; Kardos, J.; Yagi, H.; Ikegami, T.; Naiki, H.; Goto, Y. Heat of supersaturation-limited amyloid burst directly monitored by isothermal titration calorimetry. *Proc. Natl. Acad. Sci. U. S. A.* **2014**, *111* (18), 6654–6659.
- (7) Vekrellis, K.; Stefanis, L. Targeting intracellular and extracellular alpha-synuclein as a therapeutic strategy in Parkinson's disease and other synucleinopathies. *Expert Opin. Ther. Targets* **2012**, *16* (4), 421–432.
- (8) Thirunavukkuarasu, S.; Jares-Erijman, E. A.; Jovin, T. M. Multiparametric fluorescence detection of early stages in the amyloid protein aggregation of pyrene-labeled alpha-synuclein. *J. Mol. Biol.* **2008**, *378* (5), 1064–1073.
- (9) Celej, M. S.; Jares-Erijman, E. A.; Jovin, T. M. Fluorescent N-arylaminonaphthalene sulfonate probes for amyloid aggregation of alpha-synuclein. *Biophys. J.* **2008**, *94* (12), 4867–4879.
- (10) Yushchenko, D. A.; Fauerbach, J. A.; Thirunavukkuarasu, S.; Jares-Erijman, E. A.; Jovin, T. M. Fluorescent ratiometric MFC probe sensitive to early stages of alpha-synuclein aggregation. *J. Am. Chem. Soc.* **2010**, *132* (23), 7860–7861.
- (11) Nath, S.; Meuvis, J.; Hendrix, J.; Carl, S. A.; Engelborghs, Y. Early aggregation steps in alpha-synuclein as measured by FCS and FRET: evidence for a contagious conformational change. *Biophys. J.* **2010**, *98* (7), 1302–1311.
- (12) Roberti, M. J.; Morgan, M.; Menéndez, G.; Pietrasanta, L. a. L.; Jovin, T. M.; Jares-Erijman, E. A. Quantum Dots As Ultrasensitive Nanoactuators and Sensors of Amyloid Aggregation in Live Cells. *J. Am. Chem. Soc.* **2009**, *131* (23), 8102–8107.
- (13) Krol, S.; Macrez, R.; Docagne, F.; Defer, G.; Laurent, S.; Rahman, M.; Hajipour, M. J.; Kehoe, P. G.; Mahmoudi, M. Therapeutic benefits from nanoparticles: the potential significance of nanoscience in diseases with compromise to the blood brain barrier. *Chem. Rev.* **2013**, *113* (3), 1877–1903.
- (14) Qiao, R.; Jia, Q.; Huwel, S.; Xia, R.; Liu, T.; Gao, F.; Galla, H. J.; Gao, M. Receptor-mediated delivery of magnetic nanoparticles across the blood-brain barrier. *ACS Nano* **2012**, *6* (4), 3304–3310.
- (15) Yoffe, S.; Leshuk, T.; Everett, P.; Gu, F. Superparamagnetic iron oxide nanoparticles (SPIONs): synthesis and surface modification techniques for use with MRI and other biomedical applications. *Curr. Pharm. Des.* **2013**, *19* (3), 493–509.
- (16) Joshi, N.; Mukhopadhyay, A.; Basak, S.; De, G.; Chattopadhyay, K. Surface Coating Rescues Proteins from Magnetite Nanoparticle Induced Damage. *Part. Part. Syst. Charact.* **2013**, *30* (8), 683–694.
- (17) Yang, H. M.; Park, C. W.; Ahn, T.; Jung, B.; Seo, B. K.; Park, J. H.; Kim, J. D. A direct surface modification of iron oxide nanoparticles with various poly(amino acid)s for use as magnetic resonance probes. *J. Colloid Interface Sci.* **2012**, *391*, 158–167.
- (18) Ghosh, R.; Sharma, S.; Chattopadhyay, K. Effect of arginine on protein aggregation studied by fluorescence correlation spectroscopy and other biophysical methods. *Biochemistry* **2009**, *48* (5), 1135–1143.
- (19) Magde, D.; Elson, E.; Webb, W. W. Thermodynamic Fluctuations in a Reacting System—Measurement by Fluorescence Correlation Spectroscopy. *Phys. Rev. Lett.* **1972**, *29* (11), 705–708.
- (20) Nag, S.; Chen, J.; Irudayaraj, J.; Maiti, S. Measurement of the attachment and assembly of small amyloid-beta oligomers on live cell membranes at physiological concentrations using single-molecule tools. *Biophys. J.* **2010**, *99* (6), 1969–1975.
- (21) Liang, Y.; Lynn, D. G.; Berland, K. M. Direct observation of nucleation and growth in amyloid self-assembly. *J. Am. Chem. Soc.* **2010**, *132* (18), 6306–6308.
- (22) Basak, S.; Chattopadhyay, K. Fluorescence correlation spectroscopy study on the effects of the shape and size of a protein on its diffusion inside a crowded environment. *Langmuir* **2013**, *29* (47), 14709–14717.
- (23) Tcherniak, A.; Reznik, C.; Link, S.; Landes, C. F. Fluorescence correlation spectroscopy: criteria for analysis in complex systems. *Anal. Chem.* **2009**, *81* (2), 746–754.
- (24) Sengupta, P.; Garai, K.; Balaji, J.; Periasamy, N.; Maiti, S. Measuring size distribution in highly heterogeneous systems with fluorescence correlation spectroscopy. *Biophys. J.* **2003**, *84* (3), 1977–1984.
- (25) Sarkar, S.; Chattopadhyay, K. Studies of early events of folding of a predominately beta-sheet protein using fluorescence correlation spectroscopy and other biophysical methods. *Biochemistry* **2014**, *53* (9), 1393–1402.
- (26) Frimpong, A. K.; Abzalimov, R. R.; Uversky, V. N.; Kaltashov, I. A. Characterization of intrinsically disordered proteins with electrospray ionization mass spectrometry: conformational heterogeneity of alpha-synuclein. *Proteins* **2009**, *78* (3), 714–722.
- (27) Haldar, S.; Sil, P.; Thangamuniandy, M.; Chattopadhyay, K. Conversion of Amyloid Fibrils of Cytochrome c to Mature Nanorods through a Honeycomb Morphology. *Langmuir* **2014**, DOI: 10.1021/la5029993.
- (28) Zeng, S.; Huang, Y. M.; Chang, C. E.; Zhong, W. Protein binding for detection of small changes on a nanoparticle surface. *Analyst* **2014**, *139* (6), 1364–1371.
- (29) Auffan, M.; Achouak, W.; Rose, J.; Roncato, M. A.; Chaneac, C.; Waite, D. T.; Masion, A.; Woicik, J. C.; Wiesner, M. R.; Bottero, J. Y. Relation between the redox state of iron-based nanoparticles and their cytotoxicity toward Escherichia coli. *Environ. Sci. Technol.* **2008**, *42* (17), 6730–6735.
- (30) Laurent, S.; Forge, D.; Port, M.; Roch, A.; Robic, C.; Vander Elst, L.; Muller, R. N. Magnetic iron oxide nanoparticles: synthesis, stabilization, vectorization, physicochemical characterizations, and biological applications. *Chem. Rev.* **2008**, *108* (6), 2064–2110.
- (31) Hoozemans, J. J.; Chafekar, S. M.; Baas, F.; Eikelenboom, P.; Schepers, W. Always around, never the same: pathways of amyloid beta induced neurodegeneration throughout the pathogenic cascade of Alzheimer's disease. *Curr. Med. Chem.* **2006**, *13* (22), 2599–2605.
- (32) Paleologou, K. E.; Kragh, C. L.; Mann, D. M.; Salem, S. A.; Al-Shami, R.; Allsop, D.; Hassan, A. H.; Jensen, P. H.; El-Agnaf, O. M. Detection of elevated levels of soluble alpha-synuclein oligomers in post-mortem brain extracts from patients with dementia with Lewy bodies. *Brain* **2009**, *132* (Pt 4), 1093–1101.
- (33) Cabaleiro-Lago, C.; Quinlan-Pluck, F.; Lynch, I.; Lindman, S.; Minogue, A. M.; Thulin, E.; Walsh, D. M.; Dawson, K. A.; Linse, S.

Inhibition of amyloid beta protein fibrillation by polymeric nanoparticles. *J. Am. Chem. Soc.* **2008**, *130* (46), 15437–15443.

(34) Cabaleiro-Lago, C.; Szczepankiewicz, O.; Linse, S. The Effect of Nanoparticles on Amyloid Aggregation Depends on the Protein Stability and Intrinsic Aggregation Rate. *Langmuir* **2012**, *28* (3), 1852–1857.

(35) Mukhopadhyay, A.; Joshi, N.; Chattopadhyay, K.; De, G. A facile synthesis of PEG-coated magnetite ( $\text{Fe}_3\text{O}_4$ ) nanoparticles and their prevention of the reduction of cytochrome c. *ACS Appl. Mater. Interfaces* **2011**, *4* (1), 142–149.

(36) Sweers, K. K.; van der Werf, K. O.; Bennink, M. L.; Subramaniam, V. Atomic force microscopy under controlled conditions reveals structure of C-terminal region of alpha-synuclein in amyloid fibrils. *ACS Nano* **2012**, *6* (7), 5952–5960.

(37) Szczepankiewicz, O.; Cabaleiro-Lago, C.; Tartaglia, G. G.; Vendruscolo, M.; Hunter, T.; Hunter, G. J.; Nilsson, H.; Thulin, E.; Linse, S. Interactions in the native state of monellin, which play a protective role against aggregation. *Mol. Biosyst* **2011**, *7* (2), 521–532.

(38) Colombo, M.; Carregal-Romero, S.; Casula, M. F.; Gutierrez, L.; Morales, M. P.; Bohm, I. B.; Heverhagen, J. T.; Prosperi, D.; Parak, W. J. Biological applications of magnetic nanoparticles. *Chem. Soc. Rev.* **2012**, *41* (11), 4306–4334.

(39) McClendon, S.; Rospigliosi, C. C.; Eliezer, D. Charge neutralization and collapse of the C-terminal tail of alpha-synuclein at low pH. *Protein Sci.* **2009**, *18* (7), 1531–1540.

(40) Du, H.; Chandaroy, P.; Hui, S. W. Grafted poly-(ethylene glycol) on lipid surfaces inhibits protein adsorption and cell adhesion. *Biochim. Biophys. Acta* **1997**, *1326* (2), 236–248.

(41) Gref, R.; Luck, M.; Quellec, P.; Marchand, M.; Dellacherie, E.; Harnisch, S.; Blunk, T.; Muller, R. H. 'Stealth' corona-core nanoparticles surface modified by polyethylene glycol (PEG): influences of the corona (PEG chain length and surface density) and of the core composition on phagocytic uptake and plasma protein adsorption. *Colloids Surf., B* **2000**, *18* (3–4), 301–313.

(42) Perry, J. L.; Reuter, K. G.; Kai, M. P.; Herlihy, K. P.; Jones, S. W.; Luft, J. C.; Napier, M.; Bear, J. E.; DeSimone, J. M. PEGylated PRINT nanoparticles: the impact of PEG density on protein binding, macrophage association, biodistribution, and pharmacokinetics. *Nano Lett.* **2012**, *12* (10), 5304–5310.

(43) van Vlerken, L. E.; Vyas, T. K.; Amiji, M. M. Poly(ethylene glycol)-modified nanocarriers for tumor-targeted and intracellular delivery. *Pharm. Res.* **2007**, *24* (8), 1405–1414.

(44) Blummel, J.; Perschmann, N.; Aydin, D.; Drinjakovic, J.; Surrey, T.; Lopez-Garcia, M.; Kessler, H.; Spatz, J. P. Protein repellent properties of covalently attached PEG coatings on nanostructured  $\text{SiO}_2$ -based interfaces. *Biomaterials* **2007**, *28* (32), 4739–4747.

(45) Mahmoudi, M.; Simchi, A.; Imani, M.; Shokrgozar, M. A.; Milani, A. S.; Hafeli, U. O.; Stroeve, P. A new approach for the in vitro identification of the cytotoxicity of superparamagnetic iron oxide nanoparticles. *Colloids Surf., B* **2010**, *75* (1), 300–309.